SCIENTIFIC REPORTS

OPEN

SUBJECT AREAS:
APPLIED PHYSICS
OPTICAL MATERIALS
OPTICS AND PHOTONICS
OPTICAL PHYSICS

Received
17 August 2012

Accepted
10 October 2012

Published
12 November 2012

Correspondence and requests for materials should be addressed to K.H. (k_huang@xmu.edu.cn) or J.Y.K. (jykang@xmu.edu.cn)

Surface-plasmon-enhanced deep-UV light emitting diodes based on AlGaN multi-quantum wells

Na Gao, Kai Huang, Jinchai Li, Shuping Li, Xu Yang & Junyong Kang

Department of Physics, Fujian Provincial Key Laboratory of Semiconductor Materials and Application, Xiamen University, Xiamen 361005, China.

We report the development of complete structural AlGaN-based deep-ultraviolet light-emitting diodes with an aluminum thin layer for increasing light extraction efficiency. A 217% enhancement in peak photoluminescence intensity at 294 nm is observed. Cathodoluminescence measurement demonstrates that the internal quantum efficiency of the deep-UV LEDs coated with Al layer is not enhanced. The emission enhancement of deep-UV LEDs is attributed to the higher LEE by the surface plasmon-transverse magnetic wave coupling. When the proportion of the TM wave to the Al layer increases with the Al content in the $Al_xGa_{1-x}N$ multiple quantum wells, i.e., the band edge emission energy, the enhancement ratio of the Al-coated deep-UV LEDs increases.

Deep-ultraviolet light-emitting diodes (deep-UV LEDs) with emission wavelength ranging from 200 nm to 350 nm have been a subject of great interest due to their various applications, such as in biological detection, water purification, and optical catalysis[1–3]. Although the output power of deep-UV LEDs based on nitride materials have greatly increased[4–6], deep-UV LED sources still suffer from relatively low external quantum efficiency (EQE) and emission power. Currently, the maximum EQE of deep-UV LEDs with emission wavelength from 280 nm to 320 nm (UV-B) is approximately 2%[1]. Thus, further enhancing the EQE performance of deep-UV LEDs which depends on internal quantum efficiency (IQE) and light extraction efficiency (LEE) is necessary. One important limitation for achieving high efficiency III-Nitride emitters is related to the existence of charge separation issue in the QWs resulting in significant reduction in spontaneous emission rate and internal quantum efficiency[7,8]. Recent works by using non-polar III-Nitride QWs[9] and polar III-Nitride QWs with large optical matrix elements[7,10] have been used for suppressing the charge separation issues. Recently Shatalov et al. found that the upper IQE limit increases to 70% at room temperature at a wavelength of 280 nm[4]. Therefore, the relatively low LEE has become the critical issue in improving EQE. The large difference in refractive indices results in majority of the emission light generated in the active layers being reflected back to the device[11,12]. With a refractive index as high as 2.5, the LEE of the planar GaN-based LED structure only achieves approximately 5%[13]. Another reason for the low LEE in $Al_xGa_{1-x}N$ materials lies in the optical anisotropy of $Al_xGa_{1-x}N$ alloys. The emission light generated in the active layers can only escape from the top and bottom surfaces when inside an escape cone[14]. The emitted photons in this cone can escape since the polarization of emitted light is mainly perpendicular to the crystal axis within this cone ($E \perp c$)[15–17]. However, for deep-UV LEDs using $Al_xGa_{1-x}N$ ($x>0.25$) as active layers, the most dominant emission will be photons with polarization parallel to the c axis ($E \| c$), implying that deep-UV photons can no longer be extracted easily from the escaping cone[14]. Recent work showed that the incorporation of high Al-content in the $Al_xGa_{1-x}N$ QW active region led the crossover of CH and HH valence subbands resulting in dominant TM polarized spontaneous emission and optical gain[18], which was also in agreement with recent experimental works[19]. Recent works by using AlGaN-delta-GaN QW active regions had also been used for achieving dominant TE-polarized spontaneous emission and optical gain in the deep/mid UV spectral regimes[20,21]. Thus, the UV emitters with $Al_xGa_{1-x}N$ alloy as active layers show very poor LEE. Numerous schemes have been developed to enhance the LEE of LEDs, such as photonic crystal LEDs[22,23], patterned substrate[24,25], and integrated microlens array[13,26]. Recent works by using large index contrast photonic crystal[27,28] and self-assembled microlens arrays[29,30] had also been implemented in achieving significant improvement in light extraction in GaN-based LEDs. By employing optimized designs, the selective polarization excitation for modes in LEDs had also been demonstrated for photonic crystal LEDs[31,32] and self-assembled microlens

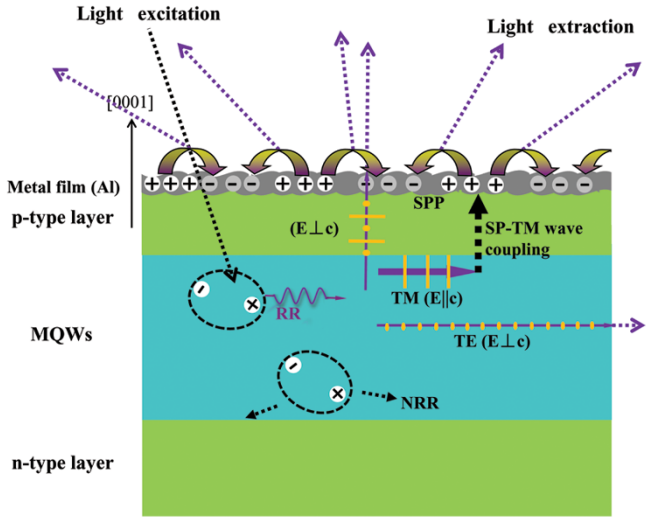

Figure 1 | A schematic illustration of the SP enhanced deep-UV LED in this study.

arrays LEDs[33]. However, for $Al_xGa_{1-x}N$ materials mostly used in deep-UV LEDs, these methods can lead to reduction of the total internal reflection caused by the high refractive index only.

Surface plasmons (SPs) have drawn great attention for their ability to enhance the light emission efficiency of LEDs, especially blue LEDs, which are waves that propagate along the surface of a conductor (usually a metal)[34–36]. The use of surface plasmon-based III-Nitride LEDs had resulted in improved IQE of the LEDs with various configurations as follow: single metallic layer[37], double metallic layers[38], and 2-D lattice arrays structures[39]. The uses of double-metallic layers and 2-D lattice arrays in surface plasmon LEDs had resulted in more than 7-times increase and 2.5 times increase in IQE in green spectral regime. For SP-enhanced LEDs, the spontaneous emission rate can be dramatically enhanced and lead to enhanced IQE by surface plasmon-quantum well (SP-QW) coupling[40,41]. The InGaN QW emission is dramatically enhanced after coatings with silver and gold, which are the best metals for SPs propagation[42–44]. The SP energy $\hbar\omega_{sp}$of silver and gold on GaN are approximately 2.76 eV (450 nm) and 2.2 eV (560 nm), respectively[37]. Thus, most reports related to SP-enhanced LEDs are focused on the visible light region[45–47]. However, for SP-enhanced LEDs using the SP-QW coupling mechanism, the distance of the metal-semiconductor interface and the active layers must be shorter than the SP fringing field penetration depth into the semiconductor[37]. However, for deep-UV LEDs, a high-quality p-type layer is generally 100 nm thick. The penetration depth is much shorter than the distance between the metal-semiconductor interface and the active layers. Thus, enhancing deep-UV LED performance using the SP-QW coupling mechanism is extremely difficult.

In this paper, we demonstrated that the LEE of complete structural deep-UV LEDs can be enhanced using the metal aluminum (Al) for SP coupling. The SP energy of Al on LEDs is higher than 5 eV (~250 nm). The real part of the dielectric constant is negative over the whole wavelength region for UV light. Thus, Al is the most ideal metal for SP coupling to deep-UV emission. Although the IQE of the LEDs are not enhanced by the SP-QW coupling, the LEE of the LEDs is enhanced by the SP-transverse magnetic (TM) wave coupling. An enhancement ratio of 217% is acquired at the wavelength of 294 nm. The enhancement ratio is higher when the band edge emission energy becomes higher. The difference of the enhancement ratio can be attributed to two effects. First, the TM wave ratio is higher at a shorter wavelength. Second, stronger coupling is expected when the photon energy is closer to the SP energy of Al on LEDs.

Results

Fig. 1 shows the designed scheme of the SP-enhanced deep-UV LED structure. A layer of 5-nm-thick Al was deposited on top of the as-grown complete structural deep-UV LED. The distance of the Al layer and the multiple quantum wells (MQWs) is approximately 100 nm, which is far beyond the SP fringing field penetration depth into the semiconductor. The penetration depth is given as follows:

$$\delta_d = \frac{1}{k_0}\left|\frac{\varepsilon_d+\varepsilon_m'}{\varepsilon_d^2}\right|^{1/2} = \frac{\lambda}{2\pi}\left|\frac{\varepsilon_d+\varepsilon_m'}{\varepsilon_d^2}\right|^{1/2}$$

where ε_d and ε_m' represent the real permittivity of dielectric material and metal, respectively[48]. In our case, Z=36 nm is calculated as the wavelength of 294 nm for Al on GaN. Obviously, the calculated penetration depth is unable to match the SP-QW coupling requirement. Thus, the energies of electron-hole pairs in MQWs cannot transfer to the interface of the Al/GaN layer to generate SPs. Therefore, the IQE of the light emitters cannot increase by SP-QW coupling. The electron-hole pairs will recombine and produce photons in the MQWs directly. The dominant band edge emission in high Al-content $Al_xGa_{1-x}N$ alloys has an E||*c* polarization orientation[15], which implies that UV light extracted from the escaping cone is very weak. As Fig. 1 shows, only part of the light wave with E⊥*c* polarization orientation can be extracted from the escaping cone. The other part of the light wave with E⊥*c* polarization orientation and the entire light wave with E||*c* polarization orientation transmits along a perpendicular direction to the *c* axis, i.e., parallel to the Al layer deposited on top of the LED. These light waves are TE and TM waves for the Al layers, respectively. Thus, the dominant band edge emission in high Al-content $Al_xGa_{1-x}N$ alloys is the TM wave for the Al layer[49,50]. The top surface of the deep-UV LEDs is not perfectly flat because of the large mismatches of the sapphire substrate, the $Al_xGa_{1-x}N$ layers, and the p-GaN contact layer. The AFM image of the top surface of the deep-UV LEDs is shown in Fig. 2 (a). The TM wave with photon energy close to the electron vibration energy of SP at the metal-semiconductor surface can be coupled by the Al layer and generate SPs[51]. The Al layer is extremely thin and the top surface of the Al layer is not perfectly flat either (As shown in Fig. 2 (b)), thus the SPs will propagate through the Al layer, recombine, and then emit light efficiently. Through these steps, the LEE of the deep-UV LEDs is enhanced by the SP-TM wave coupling.

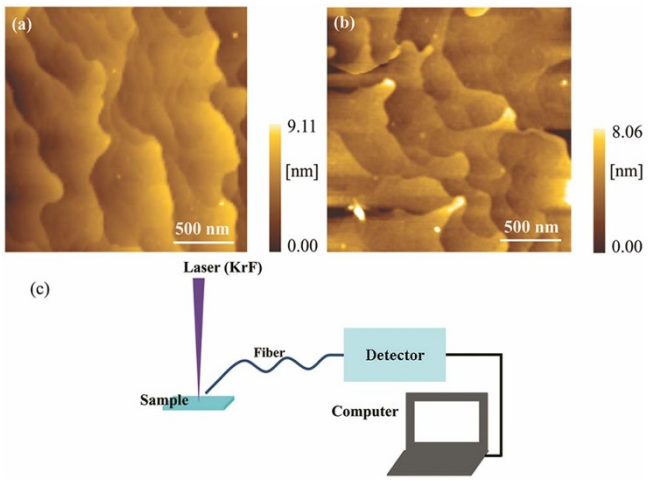

Figure 2 | The AFM images and the scheme of the PL measurement. The AFM image of the top surface of the deep-UV LEDs (a), the AFM image of the top surface of the Al layer (b) and the scheme of the PL measurement (c). The surface mean roughness of the top surface of the deep-UV LEDs and the top surface of the Al layer were 0.98 and 1.19 nm, respectively, measured by AFM over a scan area of 4 μm^2.

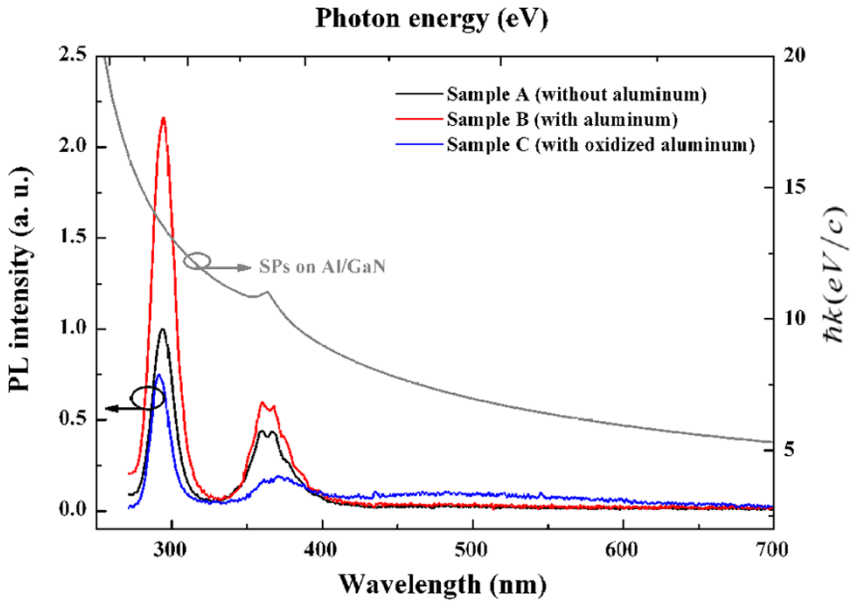

Figure 3 | Photoluminescence measurements. PL spectra of the deep-UV LED samples without (black line), with (red line) a 5-nm-thick Al layer deposited on the surfaces, with an oxidized Al layer with a 5-nm Al thickness before oxidation (blue line), and dispersion diagram of surface plasmons generated on Al/GaN surface (gray line). *k* is the SP wave vector.

Fig. 3 demonstrates the typical photoluminescence (PL) spectra of our grown deep-UV LED samples without (sample A) a 5-nm-thick Al layer deposited on the sample, with (sample B) a 5-nm-thick Al layer deposited on the sample, and with an oxidized Al layer with a 5-nm Al thickness before oxidation (sample C). As Fig. 3 shows, all the spectra contain strong emission peaks at approximately 294 nm. Weak emission peaks at 365 nm representing the band emission of the GaN capping layer are also present in the spectra. The emission peak of sample A at 294 nm is normalized as 1, and a 217% enhancement in peak PL intensity at 294 nm is observed from sample B. For the peaks at 365 nm, an enhancement of 136% is observed from the spectra. The oxidization process of Al layer is unavoidable in air, so sample C was fabricated to determine the influence of the Al oxide layer on top of the LEDs. A suppressed PL was observed in sample C. Thus, the enhanced PL of sample B is attributed to the metal Al layer on the wafer instead of aluminum oxide. The SP dispersion diagrams on the Al/GaN interfaces calculated from the dielectric functions are also shown in Fig. 3 (right axis). At the wavelengths of 294 and 365 nm, the SP wave vectors $\hbar k$of the Al/GaN surface coating are 12.8 and 9.9 eV/c, respectively. It has been reported that the higher the SP wave vector, the stronger the SP coupling[37,40]. Thus the SP coupling at 294 nm is higher than that at 365 nm. However, the GaN capping layer is much closer to the Al layer than the MQWs. Thus the discrepancy of SP wave vectors at different wavelength might not be

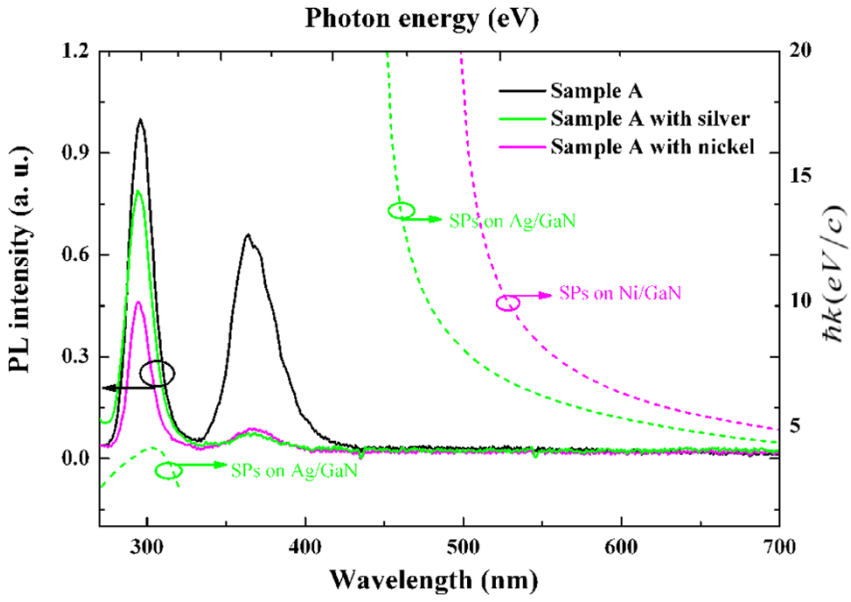

Figure 4 | Photoluminescence measurements. PL spectra of the deep-UV LED samples without (black line), with a 5-nm-thick Ag (green line) and Ni (magenta line) layer deposited on the surfaces, and dispersion diagrams of surface plasmons generated on Ag/GaN (green line) and Ni/GaN surfaces (magenta line). *k* is the SP wave vector.

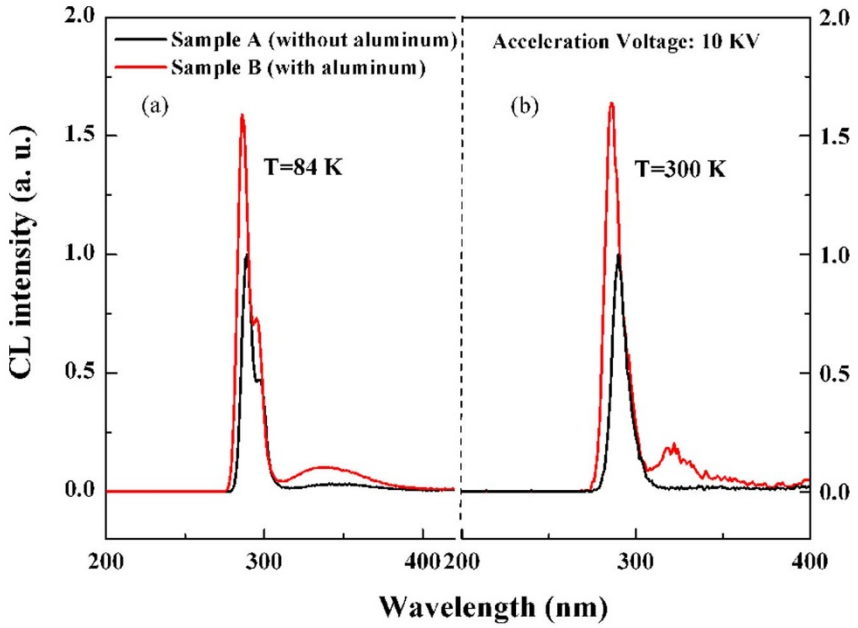

Figure 5 | Cathodoluminescence measurements. CL spectra of sample A (black line), and sample B (red line) for 84 (a) and 300 K (b). The emission peaks of sample A at 289 nm for 84 and 300 K are normalized as 1 separately.

the only reason for the difference of the enhancement ratio. The higher proportion of the TM wave at 294 nm should be another reason.

Fig. 4 shows the PL spectra of Ag- and Ni-coated deep-UV LEDs and the related dispersion diagrams of SPs on Ag/GaN and Ni/GaN. At the emission wavelength of 294 nm, the Ag-coated LED presents 13% suppression, whereas the Ni-coated LED presents 54% suppression (left axis). At the emission wavelength of 365 nm, the PL suppressions are almost the same for the Ag- and Ni-coated LEDs. These results can be explained by the SP dispersion diagrams. At the emission wavelength of 365 nm, the SP and photon energies are not matched on the Ag/GaN and Ni/GaN interfaces. At the emission wavelength of 294 nm, the SP and photon energies are not matched on the Ni/GaN interface. However, for the Ag/GaN interface, the SP wave vector $\hbar k$ is calculated as 2.6 eV/c (right axis), indicating that weak coupling exists between the photons and the Ag layer. At the emission wavelength of 294 nm, the suppression of the Ag-coated LED is not as much as that of the Ni-coated LED, whereas at the wavelength of 365 nm, the suppressions are the same. The clear correlation between the enhancement ratio of metal-coated LEDs and the SP wave vector $\hbar k$ shown in Figs. 3 and 4 suggests that the obtained emission enhancement with Al coating is due to SP coupling.

Fig. 5 presents the cathodoluminescence (CL) spectra of samples A and B for two temperatures, 84 and 300 K. The difference of the peak wavelengths and the peak shape of CL emission versus PL emission can be attributed to the different carrier injection mechanisms. The radiative recombination efficiency of samples at 84 K is much higher than that at 300 K. If the IQE of sample B is enhanced, the enhancement ratio at 84 K should be smaller than that at 300 K[37]. As shown in Fig. 4, the enhancement ratios of sample B to sample A are almost the same at 84 and 300 K. Thus, the IQE of sample B is not enhanced.

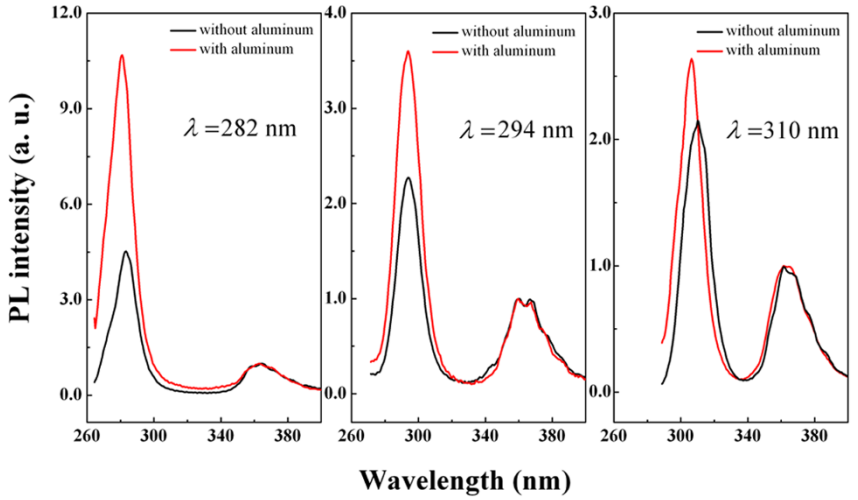

Figure 6 | Photoluminescence measurements. PL spectra of three deep-UV LEDs without (black line), with a 5-nm-thick Al (red line) layer deposited on the sample, the band edge emission wavelengths are 280 (left), 294 (middle), and 310 nm (right), respectively. The emission peak intensities at 365 nm of all Al-coated and uncoated LEDs were normalized as 1.

It's well known that $\eta_{EQE} = \eta_{IQE} \times \eta_{LEE}$[1]. The enhanced emission of sample B must be attributed to the higher LEE. Weak emission bands are also present in the wavelength range of 310 nm to 400 nm. This band might be ascribed to the deep-level emission associated with Mg acceptors or other impurities and defects[52,53]. In reference[49], emission bands exist in the wavelength range of 310 nm to 450 nm shown in the TE polarized and TM polarized in-plane electroluminescent (EL) emission of 288 nm AlGaN MQW LEDs. For the emission bands of 310 nm to 450 nm, the TM polarized EL emission is much stronger than the TE polarized EL emission, which indicates that the dominant deep-level emission is dominantly TM polarized. From the CL spectra in our experiment, the enhancement ratio of the emission bands of 310 nm to 400 nm is much larger than that of the band edge emission peak. This may indicate that the TM-polarized emission light generated in the MQWs is extracted by SP-TM wave coupling.

The proportion of the TM wave to the Al layer increases with the Al content in the $Al_xGa_{1-x}N$ MQWs, i.e., the band edge emission energy. For conventional deep-UV LEDs, this feature prevents most photons generated in the active layers from being extracted from the escaping cone. Thus, LEE is extremely low for deep-UV LEDs. However, for SP-enhanced deep-UV LEDs by SP-TM wave coupling, this feature can be an advantage. Only TM waves can be coupled with the metal layer and generate SPs, whereas TE waves cannot, thus the enhancement ratio increases with the Al content x in the $Al_xGa_{1-x}N$ MQWs.

Fig. 6 shows the PL spectra of Al-coated deep-UV LEDs with different Al contents, i.e., corresponding to different emission energies. Based on the spectra, different emission peaks exist at 281, 294, and 311 nm for different LEDs. The emission peak at 365 nm can be seen in all the PL spectra of the three LEDs. For the emission at 365 nm of the three LEDs originating from the GaN band emission with the same LED structure, the enhancement ratios at 365 nm should be the same. Thus, we normalized the emission peak intensities at 365 nm of all Al-coated and uncoated LEDs as 1 to compare the enhancement ratios of the other emission peaks. For the LED with an emission wavelength of 311 nm, the enhancement ratio is 1.23 times higher than the enhancement ratio at 365 nm. For the LEDs with an emission wavelength of 294 and 280 nm, the enhancement ratios are 1.59 and 2.36 times as strong as the enhancement ratio at 365 nm. The enhancement ratio of the Al-coated deep-UV LEDs increases when the emission wavelength becomes shorter. The wavelength-dependent enhancement ratio is attributed to two effects. First, the proportion of the TM wave of all emission light generated in the active layers is higher at a shorter wavelength, in agreement to the previous findings[18–20]. Second, coupling is stronger when the photon energy is closer to the SP energy of Al on LEDs, i.e., higher SP wave vectors at shorter wavelengths.

Discussion

In summary, this study focused on SP-enhanced, complete structural LEDs in deep-UV region, and exhibited enhancement of PL intensities using Al layers. A thin layer of Al coating can enhance the LEE of AlGaN-based deep-UV LEDs. A 217% enhancement in peak PL intensity at 294 nm is observed. CL measurement demonstrates that the IQE of the deep-UV LEDs coated with Al layer is not enhanced and the emission enhancement of sample B is attributed to the higher LEE. For the proportion of TM waves to the Al layer increases with the Al content in the $Al_xGa_{1-x}N$ MQWs and the higher SP coupling efficiency, the enhancement ratio of the Al-coated deep-UV LEDs increases when the emission wavelength becomes shorter. Compared with the other SP-enhanced LED structures using SP-QW coupling, our experiment can prevent the difficulty of meeting the metal-MQWs distance and the SP fringing field penetration depth into the semiconductor.

Methods

Fabrication. Complete structural deep-UV LED samples with emission wavelength of 294 nm (sample B) were grown on a sapphire (0001) substrate by metal-organic vapor phase epitaxy (MOVPE) in a vertical Thomas Swan system (3×2-inch CCS Aixtron). The sources were trimethylgallium (TMG), trimethylaluminum (TMA), trimethylindium (TMI), ammonia (NH_3), and H_2 as the carrier gas. Silane (SiH_4) and bis-cyclopentadienylmagnesium (Cp_2Mg) were introduced during growth for n-type and p-type doping, respectively. Based on a 1-μm-thick AlN buffer template, the LED structure consists of an approximately 1.5-μm-thick Si-doped $Al_{0.4}Ga_{0.6}N$ cladding layer, a three-period $Al_xGa_{1-x}N$ MQWs with 5-nm $Al_{0.31}Ga_{0.69}N$ well layers separated by 10-nm $Al_{0.35}Ga_{0.65}N$ barrier layers, followed by an 80-nm-thick p-type superlattice $Al_{0.3}Ga_{0.7}N/Al_{0.4}Ga_{0.6}N$ with Mg and Si $\delta-$doped, and a 10 nm p-type GaN contact layer (sample A). Subsequently, a 5-nm-thick Al layer was evaporated on top of the wafer surfaces by vacuum electron-beam deposition system (VPT CITATION ITM) for LEE enhancement (sample B). Part of sample B was annealed in O_2 atmosphere for 30 min at 450°C for comparison (sample C) to investigate the influence of the Al oxide layer. Approximately 5-nm-thick Ag and Ni coatings were deposited by a vacuum electron-beam deposition system to investigate the relationship of the SP dispersion diagrams and the enhanced PL. Deep-UV LEDs with emission wavelengths of 281 and 311 nm with and without 5-nm Al layers were also fabricated with similar structures to sample A, except for the Al composition in the active layers.

Measurements. PL measurements were carried out by exciting the MQWs with a 248 nm KrF laser at room temperature. The measurements were performed from the front surface of the metal/epitaxy layer surface. Luminescence from the front surface was collected with a spectrometer (Avaspec-2048×14). The scheme of the PL measurement is shown in Fig. 2 (c). The surface morphologies of the epilayers were investigated by an atomic force microscope (AFM, SPA400, Seiko Instruments Inc., Shizuoka, Japan). The oxidation treatment was performed in a rapid thermal annealing processor (RTP300). CL (UNISTMLT1009SEMCL) spectra of samples with and without Al layer were measured at 84 and 300 K, respectively, and were excited by an electron beam with acceleration voltages at 10 kV. The luminescence was measured with a Horiba Jobin Yvon model iHR320 imaging spectrometer system.

1. Kneissl, M. *et al.* Advances in group III-nitride-based deep UV light-emitting diode technology. *Semiconductor Science and Technology* **26**, 014036 (2011).
2. Kim, K. H., Li, J., Jin, S. X., Lin, J. Y. & Jiang, H. X. III-nitride ultraviolet light-emitting diodes with delta doping. *Applied Physics Letters* **83**, 566 (2003).
3. Taniyasu, Y., Kasu, M. & Makimoto, T. An aluminium nitride light-emitting diode with a wavelength of 210 nanometres. *Nature* **441**, 325–328 (2006).
4. Shatalov, M. *et al.* Efficiency of light emission in high aluminum content AlGaN quantum wells. *Journal of Applied Physics* **105**, 073103 (2009).
5. Khan, A. Ultraviolet light-emitting diodes based on group three nitrides. *Nature photonics* **2**, 77–84 (2008).
6. Fischer, a. J. *et al.* Room-temperature direct current operation of 290 nm light-emitting diodes with milliwatt power levels. *Applied Physics Letters* **84**, 3394 (2004).
7. Arif, R. a., Ee, Y.-K. & Tansu, N. Polarization engineering via staggered InGaN quantum wells for radiative efficiency enhancement of light emitting diodes. *Applied Physics Letters* **91**, 091110 (2007).
8. Ryou, J., Yoder, P. & Liu, J. Control of quantum-confined stark effect in InGaN-based quantum wells. *IEEE Journal of Selected Topics in Quantum Electronics* **15**, 1080–1091 (2009).
9. Farrell, R. M., Young, E. C., Wu, F., DenBaars, S. P. & Speck, J. S. Materials and growth issues for high-performance nonpolar and semipolar light-emitting devices. *Semiconductor Science and Technology* **27**, 024001 (2012).
10. Zhao, H., Liu, G., Zhang, J., Poplawsky, J. D., Dierolf, V. & Tansu, N. Approaches for high internal quantum efficiency green InGaN light-emitting diodes with large overlap quantum wells. *Optics express* **19 Suppl 4**, A991–A1007 (2011).
11. Liu, D.-S. *et al.* Light-extraction enhancement in GaN-based light-emitting diodes using grade-refractive-index amorphous titanium oxide films with porous structures. *Applied Physics Letters* **94**, 143502 (2009).
12. Fujii, T. *et al.* Increase in the extraction efficiency of GaN-based light-emitting diodes via surface roughening. *Applied Physics Letters* **84**, 855 (2004).
13. Khizar, M., Fan, Z. Y., Kim, K. H., Lin, J. Y. & Jiang, H. X. Nitride deep-ultraviolet light-emitting diodes with microlens array. *Applied Physics Letters* **86**, 173504 (2005).
14. Oder, T. N., Kim, K. H., Lin, J. Y. & Jiang, H. X. III-nitride blue and ultraviolet photonic crystal light emitting diodes. *Applied Physics Letters* **84**, 466 (2004).
15. Nam, K. B., Li, J., Nakarmi, M. L., Lin, J. Y. & Jiang, H. X. Unique optical properties of AlGaN alloys and related ultraviolet emitters. *Applied Physics Letters* **84**, 5264 (2004).
16. Morkoc, H. *et al.* Large-band-gap SiC, III-V nitride, and II-VI ZnSe-based semiconductor device technologies. *Journal of Applied Physics* **76**, 1363–1398 (1994).
17. Kawanishi, H., Senuma, M., Yamamoto, M., Niikura, E. & Nukui, T. Extremely weak surface emission from (0001) c-plane AlGaN multiple quantum well structure in deep-ultraviolet spectral region. *Applied Physics Letters* **89**, 081121 (2006).
18. Zhang, J., Zhao, H. & Tansu, N. Effect of crystal-field split-off hole and heavy-hole bands crossover on gain characteristics of high Al-content AlGaN quantum well lasers. *Applied Physics Letters* **97**, 111105 (2010).

19. Kolbe, T. *et al.* Effect of temperature and strain on the optical polarization of (In)(Al)GaN ultraviolet light emitting diodes. *Applied Physics Letters* **99**, 261105 (2011).
20. Zhang, J., Zhao, H. & Tansu, N. Large optical gain AlGaN-delta-GaN quantum wells laser active regions in mid- and deep-ultraviolet spectral regimes. *Applied Physics Letters* **98**, 171111 (2011).
21. Taniyasu, Y. & Kasu, M. Polarization property of deep-ultraviolet light emission from C-plane AlN/GaN short-period superlattices. *Applied Physics Letters* **99**, 251112 (2011).
22. Shakya, J., Kim, K. H., Lin, J. Y. & Jiang, H. X. Enhanced light extraction in III-nitride ultraviolet photonic crystal light-emitting diodes. *Applied Physics Letters* **85**, 142 (2004).
23. Oder, T. N., Shakya, J., Lin, J. Y. & Jiang, H. X. III-nitride photonic crystals. *Applied Physics Letters* **83**, 1231 (2003).
24. Bell, a. *et al.* Light emission and microstructure of Mg-doped AlGaN grown on patterned sapphire. *Applied Physics Letters* **82**, 349 (2003).
25. Wuu, D. S. *et al.* Enhanced Output Power of Near-Ultraviolet InGaN-GaN LEDs Grown on Patterned Sapphire Substrates. *IEEE Photonics Technology Letters* **17**, 288–290 (2005).
26. Lee, M. & Kuo, K. Single-step fabrication of Fresnel microlens array on sapphire substrate of flip-chip gallium nitride light emitting diode by focused ion beam. *Applied Physics Letters* **91**, 051111 (2007).
27. Matioli, E. *et al.* Polarized light extraction in m-plane GaN light-emitting diodes by embedded photonic-crystals. *Applied Physics Letters* **98**, 251112 (2011).
28. Wierer, J. J., David, A. & Megens, M. M. III-nitride photonic-crystal light-emitting diodes with high extraction efficiency. *Nature Photonics* **3**, 163–169 (2009).
29. Kumnorkaew, P., Gilchrist, J. F. & Tansu, N. Light Extraction Efficiency and Radiation Patterns of III-Nitride Light-Emitting Diodes With Colloidal Microlens Arrays With Various Aspect Ratios. *IEEE Photonics Journal* **3**, 489–499 (2011).
30. Ee, Y.-K., Arif, R. a., Tansu, N., Kumnorkaew, P. & Gilchrist, J. F. Enhancement of light extraction efficiency of InGaN quantum wells light emitting diodes using SiO_2/polystyrene microlens arrays. *Applied Physics Letters* **91**, 221107 (2007).
31. Fan, S., Villeneuve, P., Joannopoulos, J. & Schubert, E. High Extraction Efficiency of Spontaneous Emission from Slabs of Photonic Crystals. *Physical Review Letters* **78**, 3294–3297 (1997).
32. Rangel, E., Matioli, E., Choi, Y.-S., Weisbuch, C., Speck, J. S. & Hu, E. L. Directionality control through selective excitation of low-order guided modes in thin-film InGaN photonic crystal light-emitting diodes. *Applied Physics Letters* **98**, 081104 (2011).
33. Koo, W. H., Youn, W., Zhu, P., Li, X.-H., Tansu, N. & So, F. Light Extraction of Organic Light Emitting Diodes by Defective Hexagonal-Close-Packed Array. *Advanced Functional Materials* **22**, 3454–3459 (2012).
34. Barnes, W. L., Dereux, A. & Ebbesen, T. W. subwavelength optics. *Nature* **424**, 824–830 (2003).
35. Zhuang, Q., Feng, X., Yang, Z., Kang, J. & Yuan, X. Enhancement in middle-ultraviolet emission in a surface-plasmon-assisted coaxial nanocavity. *Applied Physics Letters* **93**, 091902 (2008).
36. Cai, W. & Brongersma, M. L. Nanoscale optics: Plasmonics gets transformed. *Nature nanotechnology* **5**, 485–486 (2010).
37. Okamoto, K. *et al.* Surface-plasmon-enhanced light emitters based on InGaN quantum wells. *Nature materials* **3**, 601 (2004).
38. Zhao, H., Zhang, J., Liu, G. & Tansu, N. Surface plasmon dispersion engineering via double-metallic Au/Ag layers for III-nitride based light-emitting diodes. *Applied Physics Letters* **98**, 151115 (2011).
39. Lu, C.-H., Lan, C.-C., Lai, Y.-L., Li, Y.-L. & Liu, C.-P. Enhancement of Green Emission from InGaN/GaN Multiple Quantum Wells via Coupling to Surface Plasmons in a Two-Dimensional Silver Array. *Advanced Functional Materials* **21**, 4719–4723 (2011).
40. Neogi, A. *et al.* Enhancement of spontaneous recombination rate in a quantum well by resonant surface plasmon coupling. *Physical Review B* **66**, 153305 (2002).
41. Okamoto, K. *et al.* Surface plasmon enhanced spontaneous emission rate of InGaN/GaN quantum wells probed by time-resolved photoluminescence spectroscopy. *Applied Physics Letters* **87**, 071102 (2005).
42. Chan, G. H., Zhao, J., Schatz, G. C. & Duyne, R. P. V. Localized Surface Plasmon Resonance Spectroscopy of Triangular Aluminum Nanoparticles. *Journal of Physical Chemistry C* **112**, 13958–13963 (2008).
43. Fujiki, a. *et al.* Enhanced fluorescence by surface plasmon coupling of Au nanoparticles in an organic electroluminescence diode. *Applied Physics Letters* **96**, 043307 (2010).
44. Takahashi, Y. & Tatsuma, T. Solid state photovoltaic cells based on localized surface plasmon-induced charge separation. *Applied Physics Letters* **99**, 182110 (2011).
45. Yeh, D., Huang, C., Chen, C., Lu, Y. & Yang, C. C. Surface plasmon coupling effect in an InGaN/GaN single-quantum-well light-emitting diode. *Applied Physics Letters* **91**, 171103 (2007).
46. Gifford, D. K. & Hall, D. G. Emission through one of two metal electrodes of an organic light-emitting diode via surface-plasmon cross coupling. *Applied Physics Letters* **81**, 4315 (2002).
47. Kuo, Y. *et al.* Surface plasmon coupling with radiating dipole for enhancing the emission efficiency of a light-emitting diode. *Optics express* **19 Suppl 4**, A914–A929 (2011).
48. Barnes, W. L. Surface plasmon–polariton length scales: a route to sub-wavelength optics. *Journal of Optics A: Pure and Applied Optics* **8**, S87–S93 (2006).
49. Kolbe, T. *et al.* Optical polarization characteristics of ultraviolet (In)(Al)GaN multiple quantum well light emitting diodes. *Applied Physics Letters* **97**, 171105 (2010).
50. Kawanishi, H., Senuma, M. & Nukui, T. Anisotropic polarization characteristics of lasing and spontaneous surface and edge emissions from deep-ultraviolet ($\lambda \approx 240$) AlGaN multiple-quantum-well lasers. *Applied Physics Letters* **89**, 041126 (2006).
51. Maier, S. A. *Plasmonics: Fundamentals and Applications.* (Springer 2007).
52. Li, J., Oder, T. N., Nakarmi, M. L., Lin, J. Y. & Jiang, H. X. Optical and electrical properties of Mg-doped p-type $Al_xGa_{1-x}N$. *Applied Physics Letters* **80**, 1210 (2002).
53. Shatalov, M. *et al.* Time-resolved electroluminescence of AlGaN-based light-emitting diodes with emission at 285 nm. *Applied Physics Letters* **82**, 167 (2003).

Acknowledgement

We thank Li Chen, Kongyi Li, Weihuang Yang, Hangyang Chen, Dayi Liu and Linzhe Cui for technical assistances. This work was supported by the National Research Program of China under grant Nos. 2012CB619301, 2011CB301905, 2011CB925600, National Natural Science Foundation of China under grant No. 61108064, 61227009, 90921002 and the Fundamental Research Funds for the Central Universities (2011120143).

Author contributions

All authors planned the experiment and discussed the data. The sample was fabricated by N.G. and Y.X., the measurement was carried out by N.G. and K.H., N.G., K.H., S.P.L., J.C.L. and J.Y.K. analyzed the data, and N.G, K.H. and J.Y.K. wrote the manuscript.

Additional information

Competing financial interests: The authors declare no competing financial interests.

How to cite this article: Gao, N. *et al.* Surface-plasmon-enhanced deep-UV light emitting diodes based on AlGaN multi-quantum wells. *Sci. Rep.* **2**, 816; DOI:10.1038/srep00816 (2012).